Spectrum of Engineering Sciences
ISSN (e) 3007-3138 (p) 3007-312X Volume 3, Issue 12, 2025

A Novel Intelligent Approach for Melanoma Identification Based on Pigment Network Features

Haider Ali Arshad [1], Hareem Ayesha [2], Assad Latif [3], Salahuddin [4]

[1] School of Business and Economics (SBE), University of Management and Technology (UMT), Lahore, Pakistan.
[2] Institute of Computer Science and Information Technology, The Women University Multan, Pakistan.
[3] School of Management and Economics, North China University of Water Resources and Electric Power, Zhengzhou 450046, China
[4] Department of Computer Science, NFC Institute of Engineering and technology, Multan, Pakistan.

DOI: https://doi.org/

Keywords: Deep Learning, Melanoma Detection, Pigment Network, Diffusion

Article History
Received on 5 Nov 2025
Accepted on 22 Nov 2025
Published on 18 Dec 2025

Copyright @Author
Corresponding Author: *

hareem.ayesha@wum.edu.pk

Abstract

Early identification of melanoma, one of the most aggressive and life-threatening forms of skin cancer, plays a vital role in improving patient survival and treatment outcomes. Despite significant advancements in medical imaging, accurately distinguishing malignant skin lesions from dermoscopic images remains a complex and demanding task. Among the various diagnostic features, the pigment network is considered a key visual indicator for melanoma assessment. However, reliable extraction of pigment network patterns is often hindered by challenges such as image noise, uneven illumination, and the presence of hair artifacts, which can mask critical lesion characteristics and reduce diagnostic accuracy.

To overcome these limitations, this paper introduces a set of novel image processing techniques designed for computer-aided pigment network detection. The proposed approach focuses on improving image quality and enhancing diagnostically relevant features to support more accurate melanoma analysis. The process begins with an effective preprocessing stage that applies advanced filtering methods to suppress noise and remove unwanted hair artifacts from dermoscopic images. This step significantly enhances visual clarity and prepares the images for further analysis.

Following preprocessing, the enhanced images are transformed into binary representations, and corresponding binary masks are generated to isolate regions of interest. This conversion simplifies complex image structures and enables more precise identification of pigment network patterns. In the final stage, the system detects

pigment networks and extracts essential quantitative features, including measurements such as diameter and radius, which are important indicators for evaluating melanoma presence.
Experimental results demonstrate that the proposed method performs competitively when compared with existing state-of-the-art techniques. The system achieves an average precision of 0.89 and an average recall of 0.87, with an overall classification accuracy of 88.5%. These results indicate that the proposed framework offers a reliable, efficient, and practical solution for automated pigment network detection and has strong potential to support early melanoma diagnosis in clinical settings.

INTRODUCTION

Skin cancer is the most common form of human cancer if melanoma, basal and squamous cell skin cancers are considered. Cancer is the second leading cause of deaths in the entire world. The annual ratios of all types of skin cancer are growing every year. World Health Organization estimates 8.8 million died due to cancer in 2015 in all over the world. Malignant melanoma, the deadliest form of skin cancer, is one of the most rapidly increasing cancers in the world [1]. 101,000 peoples are dying from cancer in Pakistan per year [3]. Two main reasons of this disease are the depletion of ozone layer caused by pollution and second is the extreme exposure to sun.

Metastatic melanoma is very hard to treat, so the best treatment is still early diagnosis and prompt surgical excision of the primary cancer so that it can be fully excised while it is still localized [2]. Therefore, advances in computer-aided diagnostic methods can aid self-examining approaches based on digital images, and may significantly reduce the mortality. This thesis investigates and reviews important features of automated analysis of skin lesions using digital dermoscopic images and proposes a novel approach for automated recognition of the melanoma.

Dermoscopy is a non-invasive investigative technique which is used to see a variation of patterns and structures in skin lesions that are not visible to the naked eye. It has different names like epiluminescence microscopy (ELM), dermoscopic or skin surface microscopy. The dermoscopic procedure consists of placing oil, alcohol or even water on the surface of the lesion. These solutions make epidermis more transparent to light and eradicate part of the surface reflection. After placing the liquid, the lesion is examined using a dermoscopic, a stereomicroscope, a camera or a digital imaging system.

The objective of research is to find better and more efficient way to automatically detect early melanoma. Method focuses on preprocessing stage, analysis of color variegation, border irregularity and symmetry of malignant tumor. Addition to it, Proposed method aims is to ease the doctor role in the detection of melanoma by providing better results so that patient can be diagnosed and cure at early stage.

1. Method, and materials

Automatic detection of melanoma has received certain recent attention. A lot of work has done to detect melanoma at early stage. We proposed a new approach for classification and segmentation of skin lesion. First of all, dermoscopic images are filtered to remove unwanted hair and noise. Then segmentation is applying to extract lesion area from image. Segmentation performance is also

compared with other measures, result was appreciable. The extracted lesion part is represented by color and texture features. SVM and k-NN are used with their fusion for the purpose of classification using extracted features. Figure 1 presents the flowchart diagrams of proposed methodology.

1.1. Preprocessing

The first step in the automated analysis of skin lesion images is the preprocessing of an image. The preprocessing techniques will be different for different application based on the desired dataset of an image. The key goal of preprocessing techniques is image enhancement and image restoration.

1.1.1. Gaussian Smoothing

To remove noise of image, filtering technique known as Gaussian smoothing is applied. Gaussian filter is a non-uniform low pass filter. To perform this task, 3×3 Gaussian filter is used to smoothen the image. The degree of smoothing image is determined by the standard deviation of the Gaussian. Gaussian smoothing blurs the image and removes noise and hairs. Gaussian function is given below eq (1). Where σ standard deviation of distribution and x, y is axis.

$$G(x,y)=\frac{1}{2\pi\sigma^2}e^{-\frac{x^2+y^2}{2\sigma^2}} \quad (1)$$



Original Image



Image after gaussion filter

Figure 2 Process Image

1.2. Morphological Operations

After Gaussian filtering is applied, for enhancement of filtered image, morphological operations like erosion and dilation are applied. Erosion and dilation are applied to the filtered image after Gaussian smoothing.

1.2.1. Erosion

Erosion is a morphological operation applied on image. In morphological operations, a structuring element is applied to an input image, and it creates an equal size of output image. In a morphological operation, the value of every pixel in the output image is grounded on an association of the corresponding pixel in the input image with its neighbors. In morphological erosion removes pixels on object borders. The number of pixels removed from image depends upon the size of structure element. Erosion of image *I* by a structure element *S* is denoted as eq (2).

$$I \ominus S \quad (2)$$

1.2.2. Dilation

After erosion, second morphological operation dilation is applied to image. Dilation is inverse of erosion. Dilation adds the pixel on the border of image. The value of the output pixel is the maximum value of all the pixels in the input pixel's neighborhood. In a binary image, if any of the pixels is set to the value 1, the output pixel is set to 1. Dilation of image I by structuring element S is shown below eq (3).

$$I \oplus S \quad (3)$$

1.3. Segmentation

There are many methods used for segmentation of images. The segmentation of skin lesions is a fundamental initial step in the method of automatically diagnosing melanoma. Incorrect segmentations will disturb all remaining processes like feature extraction, feature selection and the lesion detection. Region based segmentation is used for segmentation process.

1.3.1. Region Growing and Splitting

This algorithm begins with a set of "seed" points and from these; regions will grow by adding to every seed point those neighboring pixels that have same properties. At the begin image is considered as one region. It will look for groups of pixels of similar attributes and divided the image into a set of minor regions. Then a uniformity test is applied to every region: if the test fails, the region is divided into small elements. The uniformity test is applied once more; this is repeated till al1 regions are uniform, therefore splitting the image into smaller regions.



Figure 3 Example of segmented images

1.4. Feature Extractions

Features have a very significant role in the field of image processing. Feature extraction techniques are applied to acquire features which are useful for classification and recognition of images. Feature extraction techniques are useful in several image processing applications like face recognition, iris recognition, skin cancer detection etc. Behavior of an image, efficiency in classification is properties defied and observed by feature extraction. Main purpose of feature extraction is to obtain most relevant information like shape, color of an image so that it can be classified. When an input data for an algorithm is large enough for processing, then this data is transformed into reduced set of features (also called feature vector) [24]. This transferring of input into set of features is also known as feature extraction. In proposed method color and texture

features are used to present skin lesion area. Because the fact is that color and texture are only properties that dominating in the lesion area.

1.4.1. *Color Feature*

In order to measure the color existing in skin lesion, four statistics like mean, standard deviation, variance and skewness are extracted from skin lesion over individual channels of six different color spaces: RGB, HSV, YCbCr, NTSc, CIE L*u*v and CIE L*a*b. These four features are also called color moments.

Let Pi be the ith pixel of a color channel P of an image k with M pixel in color space then the four-color moments are defined as Moment 1-Mean is the average color value in channel as eq (4)

$$\mu = \frac{1}{M}\sum_{i=1}^{M} p \tag{4}$$

Moment 2- Standard deviation is the square root of variance of distribution that is written below eq (5)

$$\sigma = \sqrt{\frac{1}{M}\sum_{i=1}^{M}(Pi-\mu)^2} \tag{5}$$

Moment 3-Skewness is the measure of degree of asymmetry in the distribution as eq (6)

$$S = \sqrt[3]{\frac{1}{M}\left(\sum_{i=1}^{M}(p_i-\mu)^3\right)} \tag{6}$$

Moment 4- Variance is variation of color distribution, which is given below eq (7)

$$V = \frac{1}{M}\sum_{i=1}^{M}(p_i-\mu)^2 \tag{7}$$

The above-mentioned moments described four features which are computed over all the channels and give results in 72 color features obtained by following pattern (6 color spaces) × (3 channels for each color space) × (4 features).

1.4.2. *Texture Feature*

Texture is one of important feature used to recognize objects in an image. Image texture provides us facts about the spatial arrangement of color or intensities in an image or particular area of an image. To obtain texture features in the skin lesion, a set of statistical feature descriptor based on gray level occurrence matrix are used also abbreviated as GLCM. The GLCM functions describe the texture of an image by calculating how frequently pairs of pixels with specific values and in a specified spatial relationship take place in an image. Gray level occurrence matrix-based reports are well-known and commonly used for texture analysis of skin lesion. Co-occurrence texture features are extracted from an image in two phases. In first phase pairwise spatial concurrence of pixels is isolated by a precise angle and their distance are calculated by using gray level occurrence matrix. In second step, GLCM is used to measure a set of scalar quantities which differentiate several

features of original texture. GLCM is m × m square matrix, where m belongs to number of different gray levels in an image. The *graycomatrix* function generates a gray level co-occurrence matrix (GLCM) by computing exactly how often a pixel with the intensity value *i* occurs in a precise spatial relationship to a pixel with the value *j*. By default, the spatial relationship is well-defined as the pixel of interest and the pixel to its adjacent right (horizontally adjacent), but other spatial relationships between the two pixels can also be specified. Each element (*i*,*j*) in the resultant GLCM is basically the sum of the number of times that the pixel with value *i* occurred in the identified spatial relationship to a pixel with value *j* in the input image.

1.5. kNN and SVM classifier

In classification, kNN is a technique for classifying grounded on closest training samples in the feature space. It is the well-known and modest of all algorithms for predicting the class of a test example. kNN provide class labels at the end results. It predicts the class label, according to nearest neighbor of point of interest. This algorithm holds next three steps to classify.

- First of all, calculate distance of all training vector to test vector
- Then its picks the k closet vector
- Calculate average

If value of k is chosen 1, object is assigned the label of its nearest neighbor. The best value for k depends upon data. Generally, if larger value of k decreases the noise effect but also make boundaries among classes less different. In order to calculate the distance of training vector to test vector distance measure such as Euclidean distance, City block distance, and correlation can be used. Most common distance measure is Euclidean distance. The accuracy of kNN algorithm can be degraded in the presence of noise or irrelevant features. Training phase of kNN consist of storing the feature vector and class label of training data.

SVM stands for Support Vector Machine, it was proposed by Cortes and Vapnik in 1993. It is a powerful supervised learning tool for classification. SVM is supervised learning algorithm which is characterized by considerable resistance to over fitting, a long standing and inherent problem algorithm. This excessive feature of SVM is the fact that it pays structural risk minimization problem rather than empirical risk minimization process, which reduces the upper bound on generalization error. Generally, the SVM is considered for dichotomic classification (binary classification problem with two classes). So, the final aim of SVM is to find the optimal dichotomic hyper plane that can maximize the margin of two classes. To achieve this purpose, on both side of this hyper plane, two parallel hyper planes are created. Then, SVM attempts to discover the splitting hyper plane that make the most of the distance between the two parallel hyper planes. Instinctively an optimized hyper plane separation having largest distance is achieved. In the proposed approach, two classes of lesion are created. The SVM classifier with radial basis function (also called RBF) kernel and default parameters is trained using local features extracted from skin lesion images. Use of RBF kernel rather than other kernel has benefited that it limit training data to lie in specific boundary. It's another advantage is that it has lesser computational and numerical difficulties. Finally, in test phase, unseen skin lesion sample is given to train SVM for the purpose of classification based on extracted local features. For multiclass SVM we have considered chi-square kernel in the form of Equation 3-8, here X, Y are N dimensional inputs and K is the

kernel function that maps the data from N dimensional space to M dimension space, usually M is much larger than N . Studies show that if features are in the form of a histogram, the Chi-square kernel yields better performance as compared to the others kernels [29].

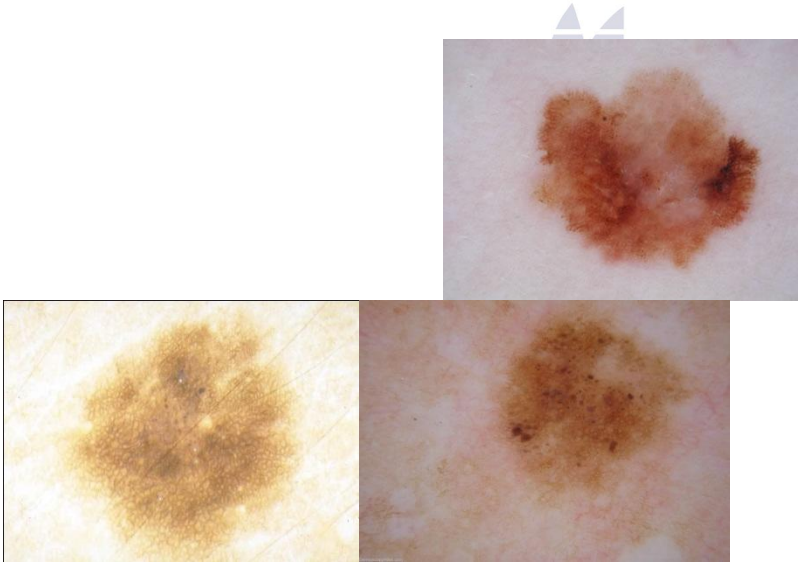
$$K(X,Y) = \sum_i x_i \frac{y_i}{x_i + y_i} \quad (8)$$

2. Implementation and result

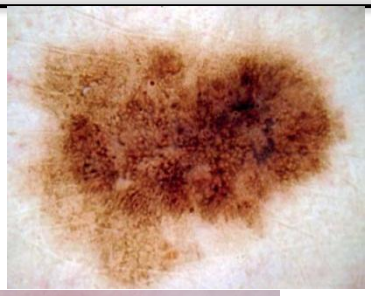
In this section, experimental results are presented in order to demonstrate the performance of proposed system. To assess the performance of proposed approach, different experiments have been carried out at large data set. The proposed algorithm is implemented in MATLAB 8.1.0 (R2013a) and the performance of proposed algorithm is evaluated through various validity measures.

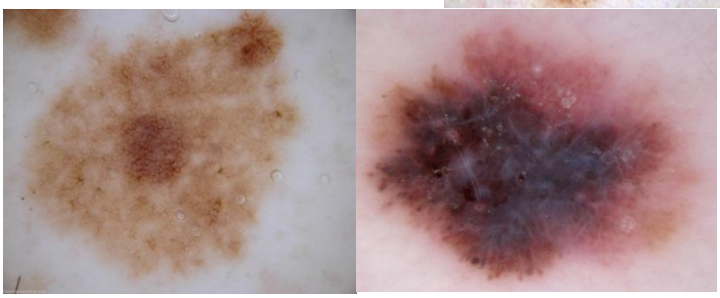
2.1. Dataset Detail

This research utilized data set [7, 27, 28] publicly available to test the proposed methodology. To evaluate the performance of proposed approach, different experiments have been carried out at large data set of digital images acquired from different sources. Figure 4 presents the samples imaged of dataset.



(a) (b) (c)



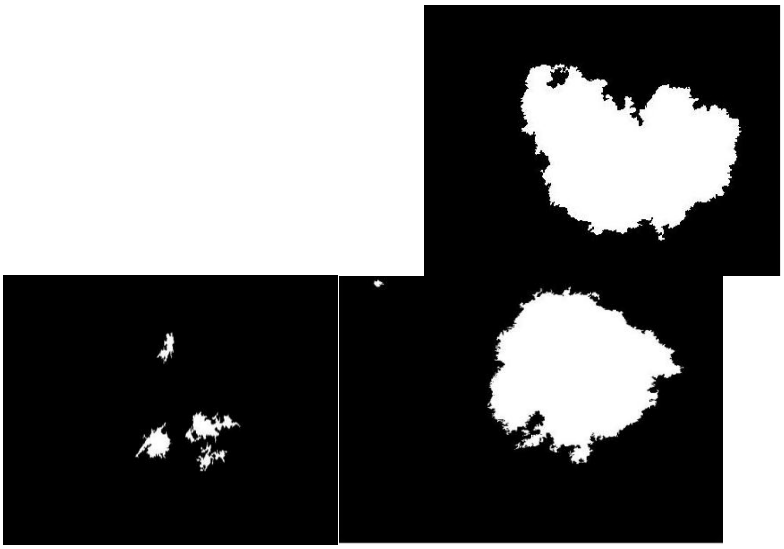


(d) (e) (f)

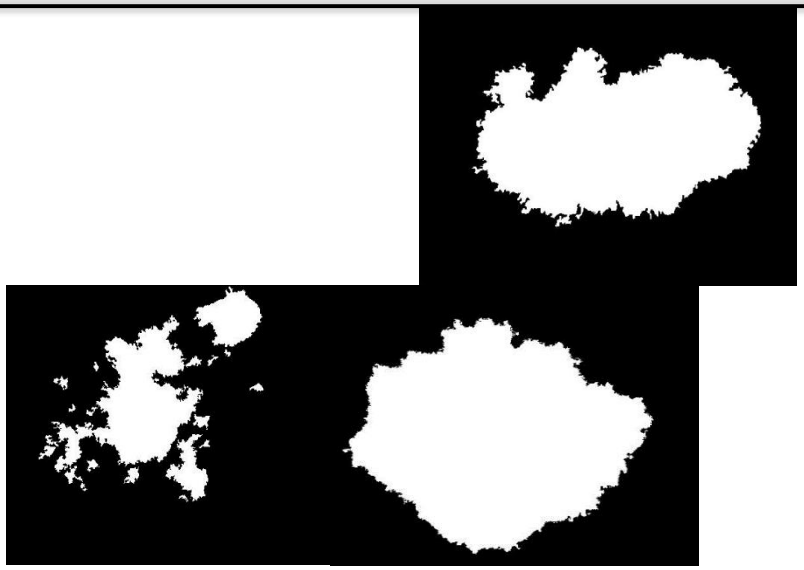
Figure 4 Example of original images

2.2. Performance analysis on dermoscopic image

The experimental work is carried out on various dermoscopy images to analyze the performance of proposed algorithm and results are compared with other algorithms. Figure 5 presents the a is gray scale image of original image (a), b is gray scale mage of original image (b), c is the gray scale image of original image (c), d is the gray scale image of original image (d), e is gray scale image of original image (e), f is gray scale image of original image.



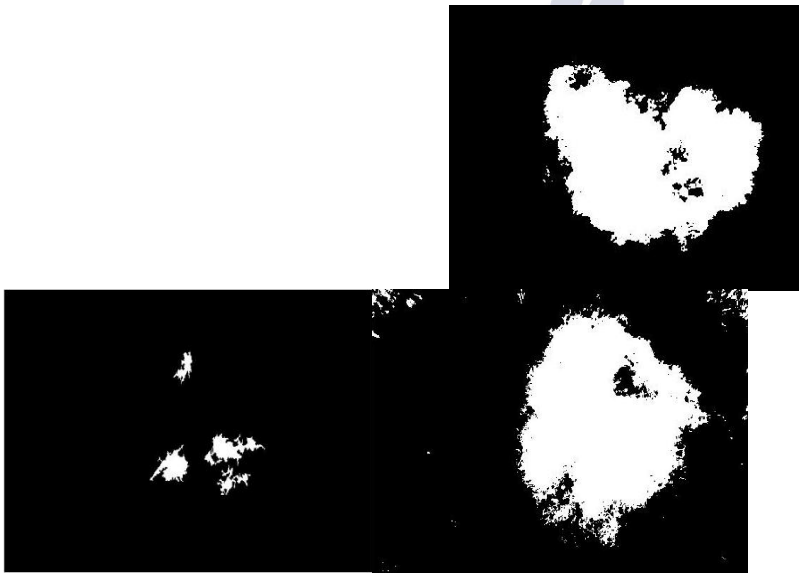
(a) (b) (c)



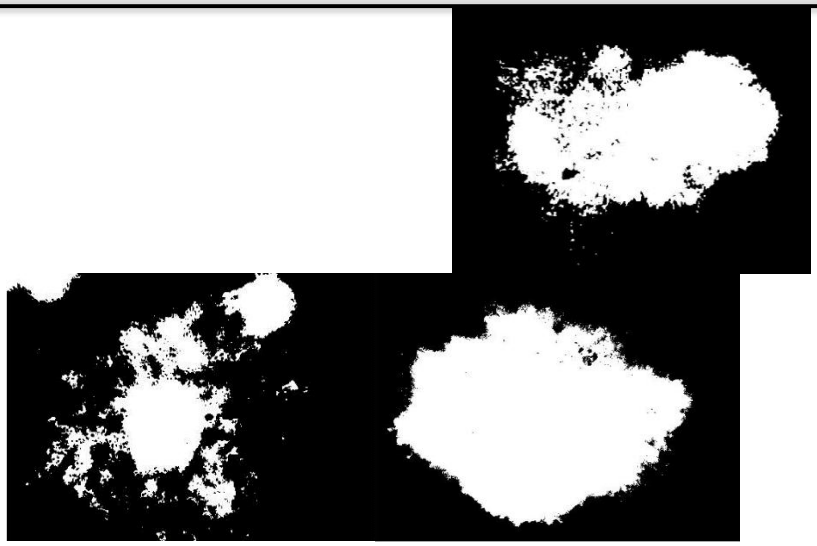
(d) (e) (f)

Figure 5 Example of gray Scale images

Figure 6 presents the binary image of original image (a), b is the binary image of original image (b), c is the binary image of original image (c), d is the binary image of original image (d), e is the binary image of 4-1(e), f is the binary image of original image (f).



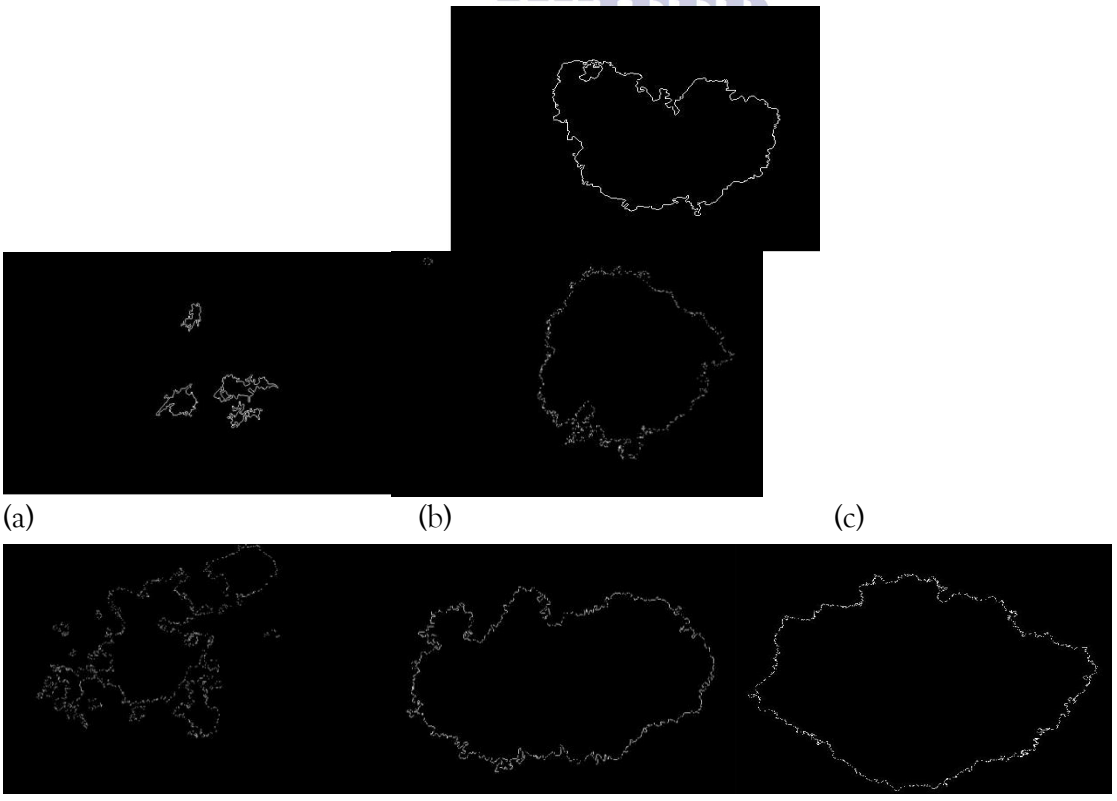
(a) (b) (c)



(d) (e) (f)

Figure 6 Example of binary Scale images

After converting melanoma image to binary image, binary mask for images is generated as shown below Figure 7. Figure presents the binary mask of image original image (a), b is the binary mask of image original image (b), c is the binary mask of image original image (c), d is the binary mask of image original image (d), e is the binary mask of image 4-3(e), f is the binary mask of image original image (f).

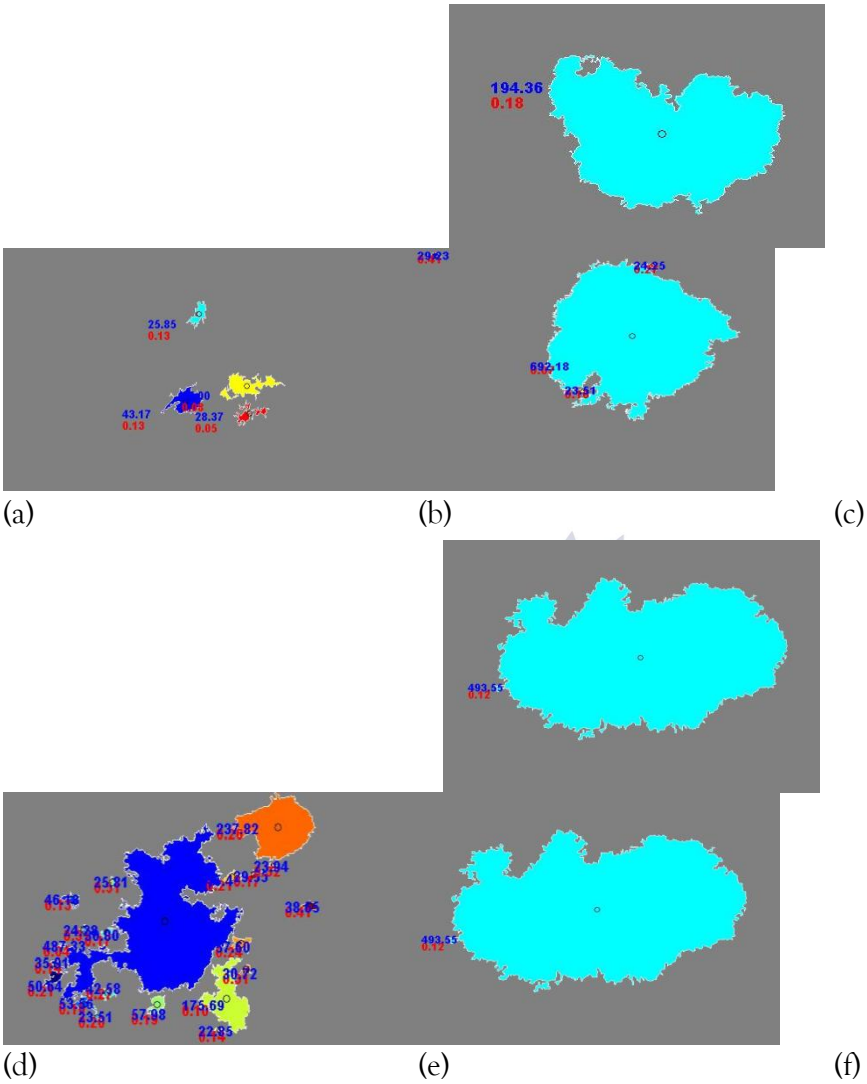


(a) (b) (c)

(d) (e) (f)

Figure 7 Example of binary Mask images

Figure presents metric calculated for image 4-4(a), b is metric calculated for image original image (b), c is metric calculated for image original image (c), d is metric calculated for image original image (d), e is metric calculated for image 4-4(e), f is metric calculated for image original image (f).



(a) (b) (c)

(d) (e) (f)

Figure 8 Example of metric calculated images

Metric is calculated on the basis of roundness and diameter. In figure 8 metric is calculated for all images. Metric value greater than 60 indicates that melanoma is detected.

The Haralick's texture features are statistics calculated on grey level co-occurrence matrix derived from each image. Table 1 shows the obtained results for Haralick features on dataset.

Table 1 Classification Performance of Haralick's on Dataset

Number of Features	Accuracy Rate
286	71%

SIFT (Scale Invariant Feature Transform) extracts texture features from an image. Table 2 shows the obtained results for SIFT and DSIFT (Dense SIFT) on dataset.

Table 2 Classification Performance of SIFT on Dataset

Vocabulary Size	Number of Features	Accuracy of DSIFT	Accuracy of SIFT
100	100	52.5%	50.3%
300	300	59.3%	56.1%
500	500	61.5%	58.0%
700	700	63.0%	59.2%
900	900	62.5%	59.3%
Combined Vocabulary (100+300+500+900)	1800	66.7%	63.1%

Experiments for LTP carried using the same number of neighbors and same size of radius as in the case of the local binary pattern (LBP). Table 4.3 describes the classification results for LTP.

Table 3 Classification Performance of LTP

Radius	Neighbors	Number of Features	Accuracy Rate
1	8	118	38.0%
2	16	486	47.3%
2	24	1110	51.3%
3	24	1110	53.4%
Combined	Combined	2824	55.0%

IBER Institute for Excellence in Education & Research

Combined color histogram for all the three-color channels obtained 29.2%. Table 3 describes the obtained results for the color histogram.

Table 3 Classification Performance of Color Histogram

Number of Features	Accuracy Rate
768	29.2%

Table 4 shows the average performance of the proposed model in term of accuracy, precision, recall and F-score

Overall Accuracy	Average Precision	Average Recall	Average F Score
85.5	0.87	0.89	86.90

The performance of proposed framework is compared with other frameworks mentioned in the literature. Comparison with existing approaches shows that our proposed method provides better results. Leo et al. [8] in 2008 get specificity and sensitivity of 85% in their proposed work. Alcon et

al. [10] get accuracy of 84% with a sensitivity of 94%, and specificity of 68%. Barata et al. [12] get specificity and sensitivity of the system is 82.1% and 91.1%. Christensen et al. [14] get accuracy of 77%. Lyatomi et al. [19], their system achieves sensitivity of 85.9% and specificity of 86%. Proposed System provides the precision of .87 and recall of .89. Our proposed system provides accuracy of 85.5%.

3. Conclusion

In this work, an improved procedure for detection of melanoma is proposed based on pigment network in dermoscopic images. Initially image is converted into gray scale image and then into binary image. Binary mask is created for binary image and then it is changed into final binary mask to detect melanoma by calculating its diameter and radius. At the end pigmented network present in the skin lesion images is detected. Feature extracted are also described with their accuracy. Haralick features have accuracy of 71%. SIFT and DSIFT features have accuracy of 63 and 66.7% respectively. Local ternary pattern features have accuracy of 55% and color histogram features have accuracy of 29.2%. Average precision was .89 and average recall was .87. The experiments are carried out on various dermoscopic images in order to check algorithm's efficiency. Proposed method shows the overall accuracy of 85.5%. In future, more features will be extracted in order to improve the algorithm's detection and accuracy for melanoma diagnosis.

REFERENCES

1. Hekmat, A., et al., Brain tumor diagnosis redefined: Leveraging image fusion for MRI enhancement classification. Biomedical Signal Processing and Control, 2025. 109: p. 108040.
2. O. Bilal, Asif Raza, S. ur R. Khan, and Ghazanfar Ali, "A Contemporary Secure Microservices Discovery Architecture with Service Tags for Smart City Infrastructures ", VFAST trans. softw. eng., vol. 12, no. 1, pp. 79–92, Mar. 2024
3. M. Waqas, Z. Khan, S. U. Ahmed and Asif. Raza, "MIL-Mixer: A Robust Bag Encoding Strategy for Multiple Instance Learning (MIL) using MLP-Mixer," 2023 18th International Conference on Emerging Technologies (ICET), Peshawar, Pakistan, 2023, pp. 22-26.
4. Khan, M.A., Khan, S.U.R. & Lin, D. Shortening surgical time in high myopia treatment: a randomized controlled trial comparing non-OVD and OVD techniques in ICL implantation. BMC Ophthalmol 25, 303 (2025). https://doi.org/10.1186/s12886-025-04135-3
5. Mahmood, F., Abbas, K., Raza, A., Khan,M.A., & Khan, P.W. (2019). Three Dimensional Agricultural Land Modeling using Unmanned Aerial System (UAS). International Journal of Advanced Computer Science and Applications (IJACSA) [p-ISSN : 2158-107X, e-ISSN : 2156-5570], 10(1).
6. Waqas, M., Bandyopadhyay, R., Showkatian, E., Muneer, A., Zafar, A., Alvarez, F. R., ... & Wu, J. (2025). The Next Layer: Augmenting Foundation Models with Structure-Preserving and Attention-Guided Learning for Local Patches to Global Context Awareness in Computational Pathology. arXiv preprint arXiv:2508.19914.
7. Khan, U. S., Ishfaque, M., Khan, S. U. R., Xu, F., Chen, L., & Lei, Y. (2024). Comparative analysis of twelve transfer learning models for the prediction and crack detection in concrete dams, based on borehole images. Frontiers of Structural and Civil Engineering, 1-17.

8. Bilal, Omair, Arash Hekmat, Inzamam Shahzad, Asif Raza, and Saif Ur Rehman Khan. "Boosting Machine Learning Accuracy for Cardiac Disease Prediction: The Role of Advanced Feature Engineering and Model Optimization." The Review of Socionetwork Strategies (2025): 1-30.
9. Khan, S. U. R., & Khan, Z. (2025). Detection of Abnormal Cardiac Rhythms Using Feature Fusion Technique with Heart Sound Spectrograms. Journal of Bionic Engineering, 1-20.
10. Khan, Saif Ur Rehman, Asif Raza, Inzamam Shahzad, and Ghazanfar Ali. "Enhancing concrete and pavement crack prediction through hierarchical feature integration with VGG16 and triple classifier ensemble." In 2024 Horizons of Information Technology and Engineering (HITE), pp. 1-6. IEEE, 2024.
11. Muneer, A., Waqas, M., Saad, M. B., Showkatian, E., Bandyopadhyay, R., Xu, H., ... & Wu, J. (2025). From Classical Machine Learning to Emerging Foundation Models: Review on Multimodal Data Integration for Cancer Research. arXiv preprint arXiv:2507.09028.
12. Khan, S.U.R., Asif, S., Bilal, O. et al. Lead-cnn: lightweight enhanced dimension reduction convolutional neural network for brain tumor classification. Int. J. Mach. Learn. & Cyber. (2025). https://doi.org/10.1007/s13042-025-02637-6.
13. Khan, Z., Hossain, M. Z., Mayumu, N., Yasmin, F., & Aziz, Y. (2024, November). Boosting the Prediction of Brain Tumor Using Two Stage BiGait Architecture. In 2024 International Conference on Digital Image Computing: Techniques and Applications (DICTA) (pp. 411-418). IEEE.
14. S.ur R. Khan, Asif. Raza, Muhammad Tanveer Meeran, and U. Bilhaj, "Enhancing Breast Cancer Detection through Thermal Imaging and Customized 2D CNN Classifiers", VFAST trans. softw. eng., vol. 11, no. 4, pp. 80–92, Dec. 2023.
15. Waqas, M., Tahir, M. A., Al-Maadeed, S., Bouridane, A., & Wu, J. (2024). Simultaneous instance pooling and bag representation selection approach for multiple-instance learning (MIL) using vision transformer. Neural Computing and Applications, 36(12), 6659-6680.
16. Khan, S. U. R., Asif, S., Zhao, M., Zou, W., Li, Y., & Xiao, C. (2026). ShallowMRI: A novel lightweight CNN with novel attention mechanism for Multi brain tumor classification in MRI images. Biomedical Signal Processing and Control, 111, 108425.
17. Khan, M. A., Khan, S. U. R., Rehman, H. U., Aladhadh, S., & Lin, D. (2025). Robust InceptionV3 with Novel EYENET Weights for Di-EYENET Ocular Surface Imaging Dataset: Integrating Chain Foraging and Cyclone Aging Techniques. International Journal of Computational Intelligence Systems, 18(1), 1-26.
18. Khan, U. S., & Khan, S. U. R. (2025). Ethics by Design: A Lifecycle Framework for Trustworthy AI in Medical Imaging From Transparent Data Governance to Clinically Validated Deployment. arXiv preprint arXiv:2507.04249.
19. Khan, S. U. R., Asif, S., Zhao, M., Zou, W., Li, Y., & Xiao, C. (2026). ShallowMRI: A novel lightweight CNN with novel attention mechanism for Multi brain tumor classification in MRI images. Biomedical Signal Processing and Control, 111, 108425.
20. Waqas, M., Tahir, M. A., & Qureshi, R. (2023). Deep Gaussian mixture model based instance relevance estimation for multiple instance learning applications. Applied intelligence, 53(9), 10310-10325.
21. Al-Khasawneh, M. A., Raza, A., Khan, S. U. R., & Khan, Z. (2024). Stock Market Trend Prediction Using Deep Learning Approach. Computational Economics, 1-32.

22. HUSSAIN, S., Raza, A., MEERAN, M. T., IJAZ, H. M., & JAMALI, S. (2020). Domain Ontology Based Similarity and Analysis in Higher Education. IEEEP New Horizons Journal, 102(1), 11-16.
23. Khan, S.U.R., Zhao, M. & Li, Y. Detection of MRI brain tumor using residual skip block based modified MobileNet model. Cluster Comput 28, 248 (2025). https://doi.org/10.1007/s10586-024-04940-3
24. Raza, A., & Meeran, M. T. (2019). Routine of Encryption in Cognitive Radio Network. Mehran University Research Journal of Engineering and Technology [p-ISSN: 0254-7821, e-ISSN: 2413-7219], 38(3), 609-618.
25. Khan, S. U. R., Asim, M. N., Vollmer, S., & Dengel, A. (2025). FloraSyntropy-Net: Scalable Deep Learning with Novel FloraSyntropy Archive for Large-Scale Plant Disease Diagnosis. arXiv preprint arXiv:2508.17653.
26. Meeran, M. T., Raza, A., & Din, M. (2018). Advancement in GSM Network to Access Cloud Services. Pakistan Journal of Engineering, Technology & Science [ISSN: 2224-2333], 7(1).
27. Khan, S. U. R., Rehman, H. U., & Bilal, O. (2025). AI-powered cancer diagnosis: classifying viable (live) vs non-viable (dead) cells using transfer learning. Signal, Image and Video Processing, 19(15), 1326.
28. Bilal, O., Hekmat, A., Shahzad, I. et al. Boosting Machine Learning Accuracy for Cardiac Disease Prediction: The Role of Advanced Feature Engineering and Model Optimization. Rev Socionetwork Strat (2025). https://doi.org/10.1007/s12626-025-00190-w
29. Asif Raza, Inzamam Shahzad, Ghazanfar Ali, and Muhammad Hanif Soomro. "Use Transfer Learning VGG16, Inception, and Reset50 to Classify IoT Challenge in Security Domain via Dataset Bench Mark." Journal of Innovative Computing and Emerging Technologies 5, no. 1 (2025).
30. Khan, M. A., Khan, S. U. R., Rehman, H. U., Aladhadh, S., & Lin, D. (2025). Robust InceptionV3 with Novel EYENET Weights for Di-EYENET Ocular Surface Imaging Dataset: Integrating Chain Foraging and Cyclone Aging Techniques. International Journal of Computational Intelligence Systems, 18(1), 204.
31. Khan, Z., Khan, S. U. R., Bilal, O., Raza, A., & Ali, G. (2025, February). Optimizing Cervical Lesion Detection Using Deep Learning with Particle Swarm Optimization. In 2025 6th International Conference on Advancements in Computational Sciences (ICACS) (pp. 1-7). IEEE.
32. Raza, Asif, Inzamam Shahzad, Muhammad Salahuddin, and Sadia Latif. "Satellite Imagery Employed to Analyze the Extent of Urban Land Transformation in The Punjab District of Pakistan." Journal of Palestine Ahliya University for Research and Studies 4, no. 2 (2025): 17-36.
33. Khan, S. U. R., Asif, S., Zhao, M., Zou, W., Li, Y., & Li, X. (2025). Optimized deep learning model for comprehensive medical image analysis across multiple modalities. Neurocomputing, 619, 129182.

34. Asif Raza, Salahuddin, Ghazanfar Ali, Muhammad Hanif Soomro, Saima Batool, "Analyzing the Impact of Artificial Intelligence on Shaping Consumer Demand in E-Commerce: A Critical Review", International Journal of Information Engineering and Electronic Business(IJIEEB), Vol.17, No.5, pp. 42-61, 2025. DOI:10.5815/ijieeb.2025.05.04
35. Li, Wentao, Amgad Muneer, Muhammad Waqas, Xiaobo Zhou, and Jia Wu. "Attention-Fusion Model for Multi-omics (AMMO) Data Integration in Lung Adenocarcinoma." In International

Workshop on Computational Mathematics Modeling in Cancer Analysis, pp. 52-60. Cham: Springer Nature Switzerland, 2024.
36. Khan, S.U.R., Raza, A., Shahzad, I., Khan, S. (2025). Subcellular Structures Classification in Fluorescence Microscopic Images. In: Arif, M., Jaffar, A., Geman, O. (eds) Computing and Emerging Technologies. ICCET 2023. Communications in Computer and Information Science, vol 2056. Springer, Cham. https://doi.org/10.1007/978-3-031-77620-5_20
37. Maqsood, H., & Khan, S. U. R. (2025). MeD-3D: A Multimodal Deep Learning Framework for Precise Recurrence Prediction in Clear Cell Renal Cell Carcinoma (ccRCC). arXiv preprint arXiv:2507.07839.
38. Khan, S. U. R., Asif, S., Zhao, M., Zou, W., & Li, Y. (2025). Optimize brain tumor multiclass classification with manta ray foraging and improved residual block techniques. Multimedia Systems, 31(1), 1-27.
39. Raza, A., Salahuddin, & Inzamam Shahzad. (2024). Residual Learning Model-Based Classification of COVID-19 Using Chest Radiographs. Spectrum of Engineering Sciences, 2(3), 367–396.
40. Khan, S. U. R., Asif, S., & Bilal, O. (2025). Ensemble Architecture of Vision Transformer and CNNs for Breast Cancer Tumor Detection From Mammograms. International Journal of Imaging Systems and Technology, 35(3), e70090.
41. Raza, A., Soomro, M. H., Shahzad, I., & Batool, S. (2024). Abstractive Text Summarization for Urdu Language. Journal of Computing & Biomedical Informatics, 7(02).
42. Hekmat, A., Zuping, Z., Bilal, O., & Khan, S. U. R. (2025). Differential evolution-driven optimized ensemble network for brain tumor detection. International Journal of Machine Learning and Cybernetics, 1-26.
43. Rehman, Laiba, Humera Batool Gill, Sohaib Ahmad, and Ezza Irshad. "FROM MOLECULES TO MIND: SIMULATING THE FUTURE OF DATA STORAGE WITH DNA, GRAPHENE AND NEURAL ENCODING." Kashf Journal of Multidisciplinary Research 2, no. 10 (2025): 45-60.
44. Waqas, M., Ahmed, S. U., Tahir, M. A., Wu, J., & Qureshi, R. (2024). Exploring multiple instance learning (MIL): A brief survey. Expert Systems with Applications, 250, 123893.
45. Khan, S. U. R. (2025). Multi-level feature fusion network for kidney disease detection. Computers in Biology and Medicine, 191, 110214.
46. Khan, S. R., Asif Raza, Inzamam Shahzad, & Hafiz Muhammad Ijaz. (2024). Deep transfer CNNs models performance evaluation using unbalanced histopathological breast cancer dataset. Lahore Garrison University Research Journal of Computer Science and Information Technology, 8(1).
47. Aslam, N., Meeran, M. T., Aslam, M., Maqbool, M. S., & Saeed, B. (2025). UNDERSTANDING URBAN EXPANSION THROUGH MULTI-TEMPORAL SATELLITE DATA ANALYSIS. Kashf Journal of Multidisciplinary Research, 2(09), 252-273.
48. Hiyat, Muhammad, Muhammad Usama Javed, Maria Akhtar, and Muhammad Tanveer Meeran. "A NOVEL SEMI-SUPERVISED FRAMEWORK FOR CYBERSECURITY THREAT DETECTION IN WIRELESS SENSOR NETWORKS." Kashf Journal of Multidisciplinary Research 2, no. 10 (2025): 1-16.
49. Bilal, O., Hekmat, A., & Khan, S. U. R. (2025). Automated cervical cancer cell diagnosis via grid search-optimized multi-CNN ensemble networks. Network Modeling Analysis in Health Informatics and Bioinformatics, 14(1), 67.

50. Asim, M. N., Ibrahim, M. A., Malik, M. I., Dengel, A., & Ahmed, S. (2022). LGCA-VHPPI: A local-global residue context aware viral-host protein-protein interaction predictor. Plos one, 17(7), e0270275.
51. Khan, S. U. R., Asim, M. N., Vollmer, S., & Dengel, A. (2025). Robust & precise knowledge distillation-based novel context-aware predictor for disease detection in brain and gastrointestinal. arXiv preprint arXiv:2505.06381.
52. N. Mayumu, D. Xiaoheng, P. Mukala, S. U. R. Khan and M. U. Saeed, "Omni-V2X: A Vision-Language Model for Actionable Insights in Vehicle-to-Everything Systems," 2025 International Joint Conference on Neural Networks (IJCNN), Rome, Italy, 2025, pp. 1-8, doi: 10.1109/IJCNN64981.2025.11228491.
53. Wasim, M., Mahmood, W., Asim, M. N., & Khan, M. U. (2018). Multi-label question classification for factoid and list type questions in biomedical question answering. IEEE Access, 7, 3882-3896.
54. Khalid, Ariba, Muhammad Usama Javed, Muhammad Tanveer Meeran, Naeem Aslam, and Muhammad Fuzail. "TOWARDS SAFE AND SECURE URBAN TRANSPORTATION INTRUSION DETECTION SYSTEM FOR CONNECTED VEHICLES IN SMART CITIES." Kashf Journal of Multidisciplinary Research 2, no. 10 (2025): 17-35.
55. Yang, H., Khan, S. U. R., Bilal, O., Chen, C., & Zhao, M. (2025). CEOE-Net: Chaotic Evolution Algorithm-Based Optimized Ensemble Framework Enhanced with Dual-Attention for Alzheimer's Diagnosis. Computer Modeling in Engineering & Sciences, 145(2), 2401.
56. S. Ur Rehman Khan, O. Bilal, S. Mistry, N. Deb, M. Mahmud and M. Bhuyan, "KDLight: A Lightweight Knowledge Distillation Framework for Medical Image Classification," *2025 International Joint Conference on Neural Networks (IJCNN)*, Rome, Italy, 2025, pp. 1-8, doi: 10.1109/IJCNN64981.2025.11228615.
57. O. Bilal, S. Ur Rehman Khan, S. Mistry, N. Deb, M. Mahmud and M. Bhuyan, "Towards Efficient Pruning and Multi-Scale Feature Transformations to Uncover Medical Diseases," *2025 International Joint Conference on Neural Networks (IJCNN)*, Rome, Italy, 2025, pp. 1-8, doi: 10.1109/IJCNN64981.2025.11229047.